Control of lasing in fully chaotic open microcavities by tailoring the shape factor

W. Fang[a] and H. Cao
Department of Physics and Astronomy, Northwestern University, Evanston, Illinois 60208

G. S. Solomon
Solid-State Photonics Laboratory, Stanford University, Stanford, California 94305 and Atomic Physics Division, NIST, Gaithersburg, Maryland 20899-8423

(Received 26 September 2006; accepted 15 January 2007; published online 23 February 2007)

The authors demonstrate experimentally that lasing in a semiconductor microstadium can be optimized by controlling its shape. Under spatially uniform optical pumping, the first lasing mode in a GaAs microstadium with large major-to-minor-axis ratio usually corresponds to a high-quality scar mode consisting of several unstable periodic orbits. Interference of waves propagating along the constituent orbits may minimize light leakage at particular major-to-minor-axis ratio. By making stadium of the optimum shape, the authors are able to maximize the mode quality factor and align the mode frequency to the peak of the gain spectrum, thus minimizing the lasing threshold. © *2007 American Institute of Physics*. [DOI: 10.1063/1.2535692]

Bunimovich's stadium billiard is a well-known model for classical and quantum chaos.[1] The ray mechanics in a stadium billiard exhibits "full chaos," i.e., there are no stable periodic orbits. However, a dense set of unstable periodic orbits (UPOs) are embedded in the sea of chaotic orbits. Although the UPOs are found with zero probability in the classical dynamics, in wave (quantum) mechanics they manifest themselves in the eigenstates of the system. There exist extra and unexpected concentrations, the so-called scars, of eigenstate density near UPOs.[2] Detailed studies have been carried out on closed or almost closed stadium cavities. A dielectric stadium, however, has its entire boundary open so that refractive escape and tunneling escape of light could happen at any point on the boundary. In the past few years, lasing was realized in both scar modes and chaotic modes of semiconductor stadiums with certain major-to-minor-axis ratio.[3,4] Highly directional output of laser emission was predicted[5] and confirmed in polymer stadiums.[6] However, not only output directionality but also low lasing threshold is required for many applications of microlasers.

In this letter, we demonstrate that low lasing threshold can be obtained in a semiconductor microstadium by controlling its shape. Contrary to common expectation, modes of such a completely open fully chaotic microcavity may have long lifetime. These special modes are typically scar modes.[7,8] When such a mode consists of several UPOs, the interference of partial waves propagating along the constituent orbits may minimize light leakage at certain major-to-minor-axis ratio.[7] Thus by tailoring the stadium shape, we are able to achieve optimum light confinement in a dielectric microstadium and thus a low lasing threshold.

The sample was grown on a GaAs substrate by molecular beam epitaxy. The layer structure consists of 500 nm $Al_{0.7}Ga_{0.3}As$ and 200 nm GaAs. In the middle of the GaAs layer there is an InAs quantum well (QW) of 0.6 nm. The lower refractive index of AlGaAs layer leads to the formation of a slab waveguide in the top GaAs layer. Stadium-shaped cylinders were fabricated by photolithography and wet chemical etching. The scanning electron microscope (SEM) images show that the etched facet of top GaAs layer is smooth and almost vertical to the substrate. The major-to-minor-axis ratio of the stadiums was varied over a wide range while the stadium area remains nearly constant. The deformation of the stadium is defined as $\epsilon \equiv a/r$, where $2a$ is the length of the straight segments connecting the two half circles of radius r.

To study their lasing properties, the stadium microcavities were cooled to 10 K in a cryostat, and optically pumped by a mode-locked Ti:sapphire laser at 790 nm. The pump beam was focused by an objective lens onto a single stadium. The emission was collected by the same lens and sent to a spectrometer. Lasing was realized in most stadiums with ϵ ranging from 0.4 to 2.2 and area $\sim 70\ \mu m^2$. Figure 1(a) shows the emission spectra of eleven stadiums slightly above their lasing thresholds. As ϵ increases, the first lasing mode jumps back and forth within the gain spectrum of the InAs QW. It is not always located near the peak of the gain spectrum. At some deformation, e.g., $\epsilon = 0.94$, 1.9, the first lasing mode is far from the gain maximum at $\lambda \sim 857$ nm. A few small and broad peaks in the emission spectrum between 847 and 857 nm are due to cavity resonances. These resonances experience higher gain than the lasing mode at $\lambda \approx 847$ nm. The only reason they do not lase is that their quality (Q) factors are low. This result indicates that the lasing modes, especially the first one, must be high-Q modes. However, when the lasing mode is away from the maximum of the gain spectrum, the relatively low optical gain at the lasing frequency results in high lasing threshold. This is confirmed in Fig. 1(b), which shows that the lasing threshold strongly depends on the spectral distance between the first lasing mode and the maximum of the gain spectrum. Unlike many deformed microcavities,[9,10] the lasing threshold in a microstadium does not increase monotonically with the deformation, e.g., the lasing thresholds in stadiums of $\epsilon = 0.7$ and 2.2 are nearly the same despite their dramatically different deformations.

To investigate individual lasing modes in microstadiums, we used a narrow bandpass filter to select one lasing mode

[a]Electronic mail: wei.fang@nist.gov

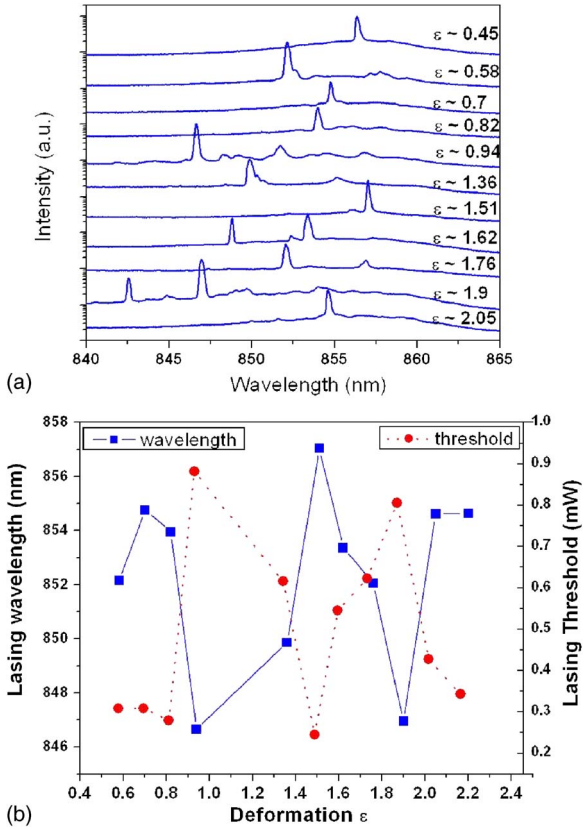

FIG. 1. (Color online) (a) Lasing spectra from 11 GaAs stadiums with different deformations. (b) Wavelength and lasing threshold of the first lasing mode as a function of ϵ.

and took its near-field image with a camera. Figure 2 shows the measurement result of a stadium with $\epsilon=1.51$. The pumping level is higher than that for the same stadium in Fig. 1(a) in order to acquire a clear near-field image. As a result, the second lasing mode appears in Fig. 2. The solid curve is the emission spectrum when the narrow bandpass filter is tuned to the first lasing mode at $\lambda=856.95$ nm. The near-field image exhibits four bright spots on the curved part of stadium boundary. We believe that these four spots represent the positions of major escape of laser light from the stadium. They can be seen from the top because of optical scattering at the boundary. However, the scattering inside the stadium is so weak that the spatial intensity distribution of lasing mode across the stadium could not be observed from the top. By tuning the bandpass filter away from cavity resonances, we took the near-field image of amplified spontaneous emission (ASE) shown as the inset B of Fig. 2. The virtually constant intensity along the curved boundary suggests that the ASE leaves the stadium mainly through the boundary of half circles instead of the straight segments. The clear difference between the near-field images of lasing mode and ASE not only confirms that the bright spots in the former are from the laser emission but also reveals that the escape routes for laser emission and ASE are distinct.

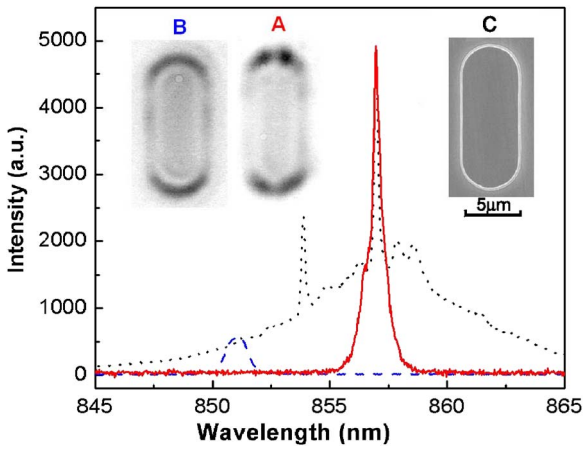

FIG. 2. (Color online) Dotted curve is the lasing spectrum from a GaAs stadium with $\epsilon=1.51$. A bandpass filter of 1 nm bandwidth selects the first lasing mode at 856.95 nm (solid curve), and inset A is the corresponding near-field image taken simultaneously. The dashed curve is the spectrum when the bandpass filter is tuned away from cavity resonances; the corresponding near-field image of ASE is shown in inset B. Top-view SEM image of the stadium is shown in inset C.

To understand the experimental results, we simulated lasing in GaAs microstadiums. The polarization measurement of laser emission from the stadium sidewall confirmed the lasing modes are transverse electric (TE) polarized. We took the effective index of refraction $n_{\text{eff}}\simeq 3.3$. The exact size and shape of the fabricated stadiums were extracted from the SEM images. Using the finite-difference time-domain (FDTD) method, we solved Maxwell's equations for electromagnetic (EM) field inside and outside a two-dimensional stadium together with the four-level rate equations for electronic populations in the InAs QW.[11] The external pumping rate for electronic populations was assumed uniform across the stadium. We gradually increased the pumping rate until one mode started lasing. Figure 3(a) shows the intensity distribution of the first lasing mode at $\lambda=850.7$ nm in the stadium with $\epsilon=1.51$. For comparison, we also calculated the high-Q modes in the passive stadium (without optical gain). By comparing the lasing mode with the resonant modes of the passive cavity, we find the first lasing mode corresponds to the highest-quality mode within the gain spectrum. As shown in Fig. 3(a), the spatial profile of the first lasing mode is almost identical to the mode at $\lambda=850.7$ nm in the passive stadium. This result illustrates that the nonlinear effect on the lasing mode is insignificant when the pumping rate is not far above the lasing threshold.

The intensity of light escaping through the stadium boundary can be approximated by the intensity just outside the boundary. From the calculated lasing mode profile, we extracted the intensity about 100 nm outside the stadium boundary. To account for the finite spatial resolution in our experiment, the output intensity distribution along the stadium boundary was convoluted with the resolution function of our imaging system. The final result (dashed curve in Fig. 4) agrees well with the measured intensity along the stadium boundary (solid curve), especially since it reproduces the positions of four bright spots in the near-field image of the lasing mode. Since there is no other mode that has similar (low) lasing threshold and output intensity profile like the measured one, we conclude that the first lasing mode observed experimentally in the stadium of $\epsilon=1.51$ corresponds to the calculated mode at $\lambda=850.7$ nm. The escape of ASE from a stadium is simulated by classical ray tracing in real space, as the interference effect is negligible due to low coherence of ASE. Following the method in Ref. 5, we calculated the intensity distribution of output rays along the boundary of a stadium with $n_{\text{eff}}=3.3$ and $\epsilon=1.51$ [dashed curve in Fig. 4(b)]. The ray-tracing result agrees with the

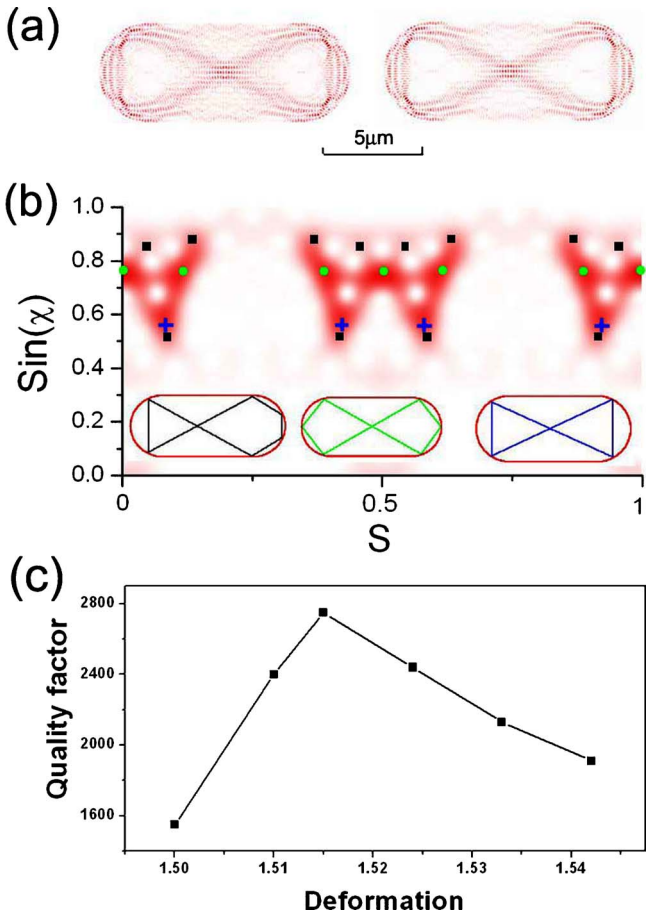

FIG. 3. (Color online) (a) Calculated intensity distribution of the first lasing mode in a stadium with $\epsilon=1.51$ (left) and the corresponding mode in the passive stadium without gain (right). Both modes have the wavelength of 850.7 nm. (b) Husimi phase space projection of the mode in (a). The horizontal coordinate s represents the length along the stadium boundary from the rightmost point, normalized by the stadium perimeter. The vertical axis corresponds to $\sin\chi$, where χ is the incident angle on the stadium boundary. The squares, dots, and crosses mark the positions of three different types of UPOs shown in the inset. (c) Q factor of the mode in (a) as a function of ϵ.

ASE intensity distribution obtained from the near-field image [solid curve in Fig. 4(b)].

To find out the classical ray trajectories that the lasing modes correspond to, we obtained quantum Poincaré sections of their wave functions. Figure 3(b) is the Husimi phase space projection of the lasing mode in Fig. 3(a), calculated from its electric field at the stadium boundary. It reveals that the lasing mode is a scar mode, and it consists mainly of three different types of UPOs plotted in the inset of Fig. 3(b). Since the constituent UPOs are above the critical line for total internal reflection, the lasing mode has long lifetime. We calculated the quality factor of this mode in passive stadium as we varied the deformation ϵ around 1.51. Its Q value first increases then decreases as ϵ increases, leading to a maximum at $\epsilon=1.515$. Such variation of quality factor is attributed to interference of waves propagating along the constituent UPOs.[7,12] The interference effect depends on the relative phase of waves traveling in different orbits. The phase delay along each orbit changes with the orbit length as ϵ varies. At some particular deformation, constructive interference may minimize light leakage out of the cavity, thus maximizing the quality factor. Since the actual deformation $\epsilon=1.51$ is nearly identical (within 0.3%) to the optimum deformation ($\epsilon=1.515$), the mode is almost at the maximum of its quality factor. Furthermore, its frequency is close to the peak of the gain spectrum. Thus the lasing threshold is minimized, as shown in Fig. 1(b).

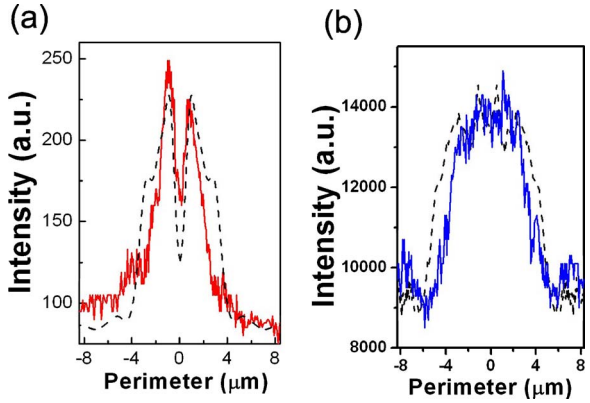

FIG. 4. (Color online) Output intensity of laser emission (a) and ASE (b) along the boundary of a GaAs stadium with $\epsilon=1.51$ and area $\simeq 70\ \mu m^2$. The range of the horizontal coordinate is half of the stadium boundary, from the center of one straight segment to the other. The solid curves are the experimental results extracted from the near-field images of the lasing mode and ASE in the insets of Fig. 2. The dashed curves are the numerical simulation results obtained with the FDTD method (a) and real-space ray tracing (b).

In summary, we demonstrated experimentally that lasing in a semiconductor microstadium can be optimized by controlling its shape. By tuning the stadium shape to the optimum deformation, we not only optimize light confinement in the stadium but also extract the maximum gain by aligning the mode frequency to the peak of the gain spectrum. The simultaneous realization of the lowest cavity loss and the highest optical gain leads to minimum lasing threshold of a microstadium laser. As the dielectric microstadium represents a completely open fully chaotic cavity, this work opens the door to control chaotic microcavity lasers by tailoring its shape.

The authors acknowledge Peter Braun and Gabriel Carlo for stimulating discussions. This work is supported by NIST under Grant No. 70NANB6H6162 and by NSF/MRSEC under Grant No. DMR-00706097.

[1] M. C. Gutzwiller, *Chaos in Classical and Quantum Mechanics* (Springer, Berlin, 1990), Vol. 1, p. 196.
[2] E. J. Heller, Phys. Rev. Lett. **53**, 1515 (1984).
[3] T. Harayama, T. Fukushima, P. Davis, P. O. Vaccaro, T. Miyasaka, T. Nishimura, and T. Aida, Phys. Rev. E **67**, 015207(R) (2003).
[4] T. Harayama, P. Davis, and K. S. Ikeda, Phys. Rev. Lett. **90**, 063901 (2003).
[5] H. G. L. Schwefel, N. B. Rex, G. E. Tureci, R. K. Chang, A. D. Stone, T. B. Messaoud, and J. Zyss, J. Opt. Soc. Am. B **21**, 923 (2004).
[6] M. Lebental, J. S. Lauret, R. Hierle, and J. Zyss, Appl. Phys. Lett. **88**, 031108 (2006).
[7] W. Fang, A. Yamilov, and H. Cao, Phys. Rev. A **72**, 023815 (2005).
[8] S. Y. Lee, M. S. Kurdoglyan, S. Rim, and C. M. Kim, Phys. Rev. A **70**, 023809 (2004).
[9] J. U. Nockel and A. D. Stone, Nature (London) **385**, 45 (1997).
[10] E. E. Narimanov, G. Hackenbroich, P. Jacquod, and A. D. Stone, Phys. Rev. Lett. **83**, 4991 (1999).
[11] A. S. Nagra and R. A. York, IEEE Trans. Antennas Propag. **46**, 334 (1998).
[12] T. Fukushima and T. Harayama, J. Lightwave Technol. **18**, 2208 (2000); T. Fukushima, T. Harayama, and J. Wiersig, Phys. Rev. A **73**, 023816 (2006); T. Fukushima, IEEE J. Sel. Top. Quantum Electron. **10**, 1039 (2004).